THE CESIUM BEAM FREQUENCY STANDARD NRLM-II

Y. Koga, Y. Nakadan, J. Yoda

JOURNAL DE PHYSIQUE
Colloque C8, supplément au n°12, Tome 42, décembre 1981 *page* C8-247

THE CESIUM BEAM FREQUENCY STANDARD NRLM-II

Y. Koga, Y. Nakadan and J. Yoda

National Research Laboratory of Metrology, Tsukuba Science City, Japan.

Abstract - Design and performance of the cesium beam frequency standard, NRLM-II , are reported. The interaction length 1 m is adopted from the viewpoints of the C-field homogeneity and the signal to noise ratio of resonance signal. The frequency stability is estimated as better than $8\times10^{-12}\tau^{-1/2}$ for short term and 8×10^{-14} for 1~2 days. Preliminary evaluation of accuracy is about 5×10^{-13} , and the standard frequency is estimated as $+(2\sim3\pm5)\times10^{-13}$ higher than that of TAI.

1. Introduction

The cesium beam frequency standard of the National Research Laboratory of Metrology, NRLM-II , was constructed in 1975. As the previous study on the first model, NRLM-I [1], revealed its frequency fluctuation was brought forth mainly due to two causes, i.e., for the averaging time shorter than a few hours, due to scattering of the atomic beam because of the poor vacuum of 2-3X10 Pa and, for the longer averaging time, due to the insufficiency of the magnetic shielding, great attention was paid to the construction of NRLM-II. During 1977 and 1978, the preliminary evaluations of accuracy was made. After that, the NRLM moved to a new site in Tsukuba Science City, about 60 km northeast of Tokyo, and the reconstruction of NRLM has been completed. The work is being directed toward improvement of its accuracy.

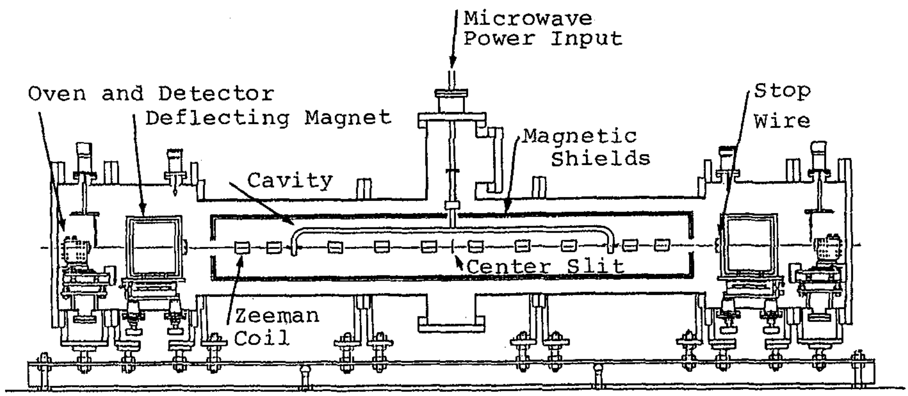

Fig.1 : The beam tube of NRLM-II

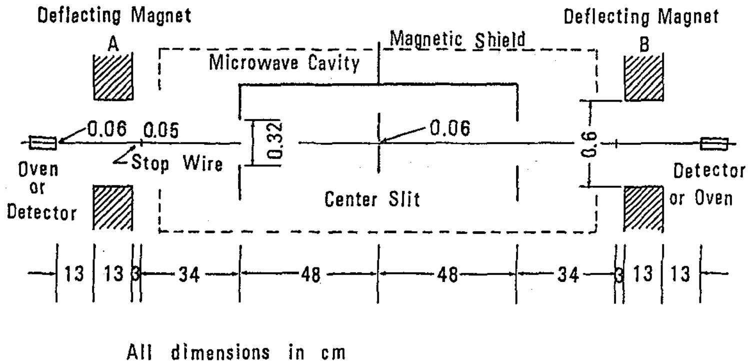

Fig.2 : Beam optics

2. Design and construction

1) Atomic beam tube

The atomic beam tube has an ordinary beam optics in axial mode with a ribbon-type beam, two deflecting magnets and a single-U type microwave cavity of which separation is approximately 1 m, and beam reversal capability. Outline of its construction and beam optics are shown in Fig.1 and Fig.2, respectively.

The vacuum chamber, 220 l in volume, is evacuated by three 500 l/s ion pumps to $3\sim4\times10^{-6}$ Pa, which is suitable for beam operation. Two slidable carriages containning a pair of oven and detector are equipped at both ends of the vacuum chamber to permit bi-directional beam operation. The oven with seven collimators in line provides a beam of 0.6 mm in width and 10 mm in hight. As an ionizer of the detector an 80%Pt 20%Ir ribbon is employed. In order to prevent a contamination by cesium metal, graphite plates are set in places.

To provide a highly homogeneous C-field and to keep a high vacuum as well, particular attention was paid to the selection of materials in the C-field region. Aluminum, phospher bronze and copper were used for various elements inside of the magnetic shield, and stainless steel for the others. Porcelain and glass were used for the electric insulator. Three magnetic shields of rectangular section are assembled around the interaction region. They are made of mu-metal plate of 2 mm thick, and the length is about 1.5 m. As was reported elsewhere 2), the peak to peak variation of the residual field along the beam path was less than 2×10^{-3} A/m.

A field intensity and its gradient of the deflecting magnets at the beam axis are 6.8×10^{5} A/m and 7.2×10^{5} A/m/cm, respectively. They are enclosed with double magnetic shields, the inner one is of soft iron, the outer mu-metal, in order to prevent the leakage flux from disturbing the C-field. A stop wire of 0.5 mmϕ is attached on each outer shield of the deflecting magnets.

The microwave cavity is composed of a central E-plane tee and two arms with beam holes. Adjusting procedure is similar to that of NRC 3). Two arms are tuned at the right frequency separately, and the tee is so adjusted that the electrical center is located at the center of the tee by observing the input VSWR. Then, fine tuning is made after having assembled them as a U-type cavity.

2) Control electronics

The system used for excitation of the cesium resonance in the

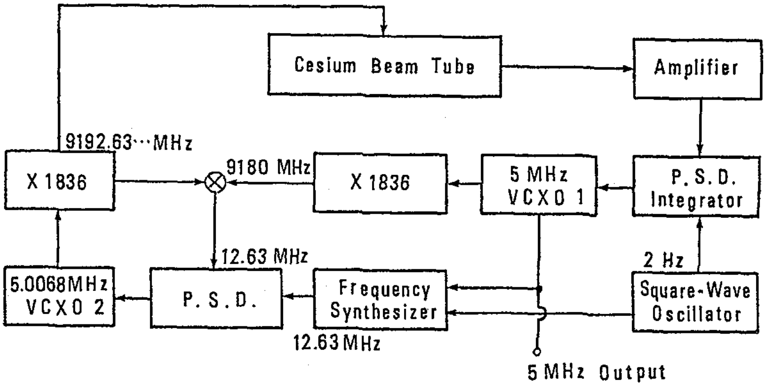

Fig.3 : The block diagram of the control electronics

NRLM-II is shown in Fig.3. The single control loop system which consists of two Voltage Controlled Oscillators(5.000 MHz VCXO1 and 5.0068 MHz VCXO2) and a commercial frequency synthesizer is adopted so that the resonant frequency is easily measured. The microwave signal which is applied to the cesium beam tube is produced by multiplying the output of VCXO2. This signal is also mixed with the multiplied signal of VCXO1 and the difference signal of 12.63 MHz is phase compared with the frequency synthesizer output signal. The error signal is applied to VCXO2 in such a way that phase difference is reduced to zero. So, VCXO2 is continuously phase locked to VCXO1. These crystal frequency stabilities in open loop are few parts in 10^{12} with averaging times of about 1 to 30 s. In this system, the output frequency of VCXO1 is step adjustable $1.087\mathrm{X}10^{-12}$per step of 0.01 Hz in the synthesizer.

12.63 MHz signal of the synthesizer contains the square-wave 2 Hz frequency modulation with 120 Hz in the modulation width. Therefore, 9192 MHz is also modulated by 2 Hz. This modulation signal is fed to the Phase Sensitive Detector (P.S.D.) in order to provide the reference for demodulation of the beam signal producted by the hot wire detector and operational amplifier in the vacuum chamber. The output of P.S.D. is the error signal which is integrated and fed as a control signal to VCXO1. The whole system forms a proportional control loop where the oscillator error, with reference to the cesium resonance, is reduced by increasing the servo gain. Using this modulation system, the frequency shift due to the harmonic distortion in the modulation was compared with former system of modulation by the 21 Hz sinusoidal wave. Then, sqaure wave frequency modulation has been used in the NRLM standard since 1975.

3. Performances

1) Frequency stability

Figure 4 shows the relative frequency stability between NRLM-II and an HP cesium clock with a high performance tube. In the range of the shorter averaging time up to a few hours, $\sigma_y(\tau)$ is about $7{\sim}8\mathrm{X}10^{-12}\ \tau^{-1/2}$. The F value under the present conditions (Is=15 pA, In=0.016 pA, Bn≈1 Hz, W=150 Hz) is estimated to be 13. From the F value estimation, $\sigma_y(\tau)$ is expected to be $6.5\mathrm{X}10^{-12}\ \tau^{-1/2}$. On the other hand, in the early stage of experiment with a cavity of 1.2 m

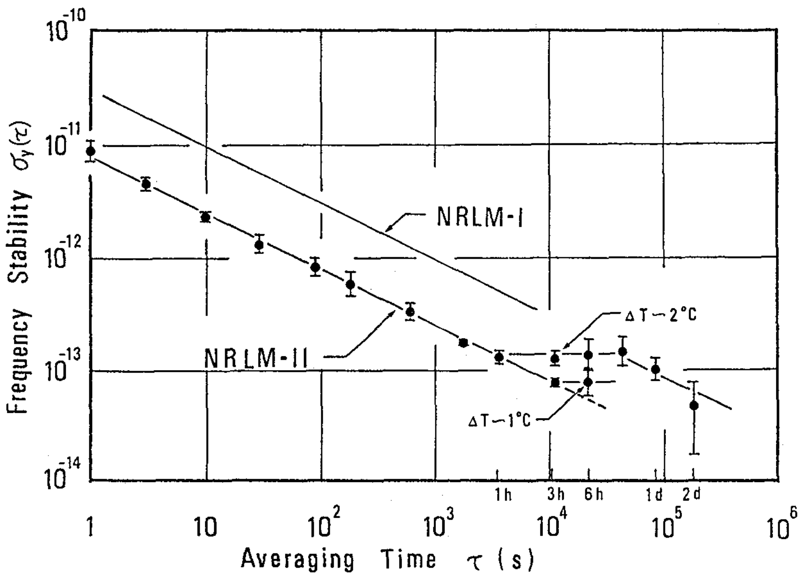

Fig. 4 : The relative frequency stability measured with respect to the HP cesium clock

length the F value was 20 for the condition (Is=20 pA, In=0.018 pA, Bn=1 Hz, W=115 Hz). It was expected that the stability could arrive at $4X10^{-12}\tau^{-1/2}$, but the measured value of $\sigma_y(\tau)$ was the same as the present one [4]. They appear to have been influenced mainly by the limitation of frequency stability imposed by the HP cesium clock rather than that of the standard itself. In the range of longer averaging time, flicker floor appears and then $\sigma_y(\tau)$ decreases for 1-2 days averaging. The value of the flicker floor depends on the diurnal change of ambient temperature in such magnitude as $8X10^{-14}$ at the fluctuation of 1 °C and $1.4X10^{-13}$ at 2 °C.

2) Accuracy evaluations

In Table 1, the various biases and their uncertainties in the frequency of NRLM-II are summarized. The bias due to the C-field intensity, normally 7.2 A/m, is obtained by measuring the transition frequencies of $(4,1)\leftrightarrow(3,1)$ and $(4,-1)\leftrightarrow(3,-1)$. Its uncertainty depends on the error of frequency measurements. The bias and uncertainty due to the inhomogeneity of the C-field are estimated from $(4,-3)\leftrightarrow(4,-4)$ transition frequencies measured by ten Zeeman coils.

The microwave power shift measurement is taken by varying the power from +1 dB to -7 dB of optimum power. The frequency and its uncertainty at zero power is determined by applying least square method to these data. The modulation shift is also measured in the same method as the power shift in the range of modulation width from 60 Hz to 140 Hz. The modulation shift is supposed to arise from two causes such as the nonlinearlity of modulation and demodulation and the asymmetry of the resonance signal. In this case, the former is proved to be major by a same measurement with an digital signal processing system which has been equipped recently.

The second order Doppler shift is calculated from

$$df = -\frac{1}{2} f_o \frac{\overline{V_D^2}}{c^2}, \qquad 5)$$

where $\overline{V_D^2}$, a mean-squared velocity, is obtained by the truncated Maxwellian method [6]. The lower and the upper velocity limits are Pmin=1.15, Pmax=1.85 for the oven temperature of 120 °C, respectively. The uncertainty of 0.5 mHz is corresponding to the error in the curve fitting.

The cavity pulling and the servo error follow worst estimations. For the power shift and the modulation shift, Table 1 shows the maximum and minimum values for the frequency bias obtained through the measurements for four conditions of the combination of the beam direction and the C-field direction. And these maximum values are adopted in the calculation of total error.

Factors	Bias(mHz)	Uncertainty(mHz)
1.Zeeman shift	3.4×10^3	0.5
2.Magnetic field inhomogeneity	0.1	0.1
3.Shift by microwave power (including cavity phase shift)	2.5～11	0.8～1.2
4.Modulation and demodulation shift	0.6～11.7	0.6～4.1
5.Second order Doppler shift	5	0.5
6.Cavity pulling	0.1	0.1
7.Servo system offset	0	0.3
Total error $\sqrt{\sum x_i^2}$		4.4

Table 1. Accuracy evaluation for NRLM-II

3) The frequency of NRLM-II relative to TAI

During the experiment of accuracy evaluations, the absolute frequency of NRLM-II was measured in terms of TAI. The measurement includes the phase comparison between NRLM-II and an HP cesium clock, the master clock of the NRLM, which is regularly compared with those of the Radio Research Laboratories (RRL) and the Tokyo Astronomical Observatory (TAO). For the reduction to the frequency of TAI, the values of $[(UTC)-(UTC)_{RRL}]$ and $[(UTC)-(UTC)_{TAO}]$ in the Annual Report of BIH are used. The results are shown in Table 2, where f_{II} and f_{TAI} are frequencies of NRLM-II and TAI, respectively.

4. Acknowledgment

The authors wish to express their appreciation to Mr. T. Inouye and Mr. M. Nara for their responsibility in the clock comparison.

Term of Measurement	$[(f_{II}-f_{TAI})/f_{TAI}] \times 10^{13}$ via RRL	via TAO
November, 1977	+2.8 ±7.2	+2.4 ±7.2
February, 1978	+2.5 ±4.8	+2.4 ±4.8
July , 1978	+2.1 ±4.9	+3.1 ±4.9

Table 2 Frequency of NRLM-II

References

1) Y. Koga, Y. Nakadan and J. Yoda : Oyo Buturi 45 (1976) 753 [in Japanese].
2) J. Yoda and Y. Koga : Oyo Buturi 45 (1976) 874 [in Japanese].
3) A.G. Mungall and H. Daams : Metrologia 6 (1970) 60.
4) Y. Koga, Y. Nakadan and J. Yoda : Japan. J. Appl. Phys. 17 (1978) 749.
5) H. Hellwig, S. Jarvis, Jr., D. Halford and H.E. Bell : Metrologia 9 (1973) 107.
6) A.G. Mungall : Metrologia 7 (1971) 49.